

## ***Supporting information***

# Designing active Ta<sub>3</sub>N<sub>5</sub> photocatalyst for H<sub>2</sub> and O<sub>2</sub> evolution reactions by specific exposed facets engineering: a first-principles study

Moussab Harb,\* Luigi Cavallo and Jean-Marie Basset

KAUST Catalysis Center (KCC), Physical Sciences and Engineering Division (PSE), King Abdullah University of Science and Technology (KAUST), Thuwal 23955-6900, Saudi Arabia

## Computational details

The spin-polarized density functional theory (DFT) with the plane wave (PW) approach was applied to optimize all bulk and slab structures using the Perdew-Burke-Ernzerhof (PBE)<sup>1</sup> exchange-correlation formalism, as implemented in VASP software.<sup>2-5</sup> The projector-augmented wave (PAW)<sup>6</sup> approach was adopted for core electrons description. The wave functions were expanded with a sufficient kinetic energy cutoff (400 eV). Benchmark tests using 500 eV energy cutoff revealed a good convergence of the bond lengths and lattice parameters from 400 eV. A suitable Monkhorst-Pack  $k$ -points mesh<sup>7</sup> was applied for each structure to carry out the reciprocal space numerical integrations to sample the Brillouin zone. The valence electrons used in the computations are  $2s^22p^3$  for N,  $2s^22p^4$  for O, and  $5d^36s^2$  for Ta. The slabs were optimized by maintaining constant the lattice vectors obtained from the bulk material. The ground-state atomic geometries were acquired by reducing the Hellmann-Feynmann forces on each species (near  $0.01 \text{ eV}\cdot\text{\AA}^{-1}$ ) and the electronic tolerance at each ionic step for each supercell (below  $10^{-6} \text{ eV}$ ). As the replacement of N by O leaves one extra electron, different spin states were examined for each stoichiometry in the case of partial O-enriched  $\text{Ta}_3\text{N}_5$  to find the most favorable configuration.

Thermal contributions of  $\text{N}_2$  and  $\text{O}_2$  as a function of temperature were computed using DMol program<sup>8</sup> with PBE and DNP basis set.<sup>9</sup> Their electronic energy together with those of solids were computed using VASP.  $\Delta\mu^{\text{N}}$  and  $\Delta\mu^{\text{O}}$  were fixed at  $p^{\text{N}_2} = p^{\text{O}_2} = 1 \text{ atm}$  and  $T = 1200 \text{ K}$  (typical annealing temperature used experimentally for this material).

From the computed density of states (DOS) using HSE06<sup>10,11</sup> with VASP on the PBE-based relaxed geometries, the electronic band gap was obtained. To reach the convergence needed for the band gaps, an increased energy cutoff until 500 eV was chosen.

As the bulk calculation does not possess an absolute reference for the electrostatic potential, the band positions can be done by modeling a material-vacuum system, where the

electronic band structure is aligned to an energy scale reference.<sup>12-16</sup> Based on the optimal thickness, a first slab calculation is needed to be performed for obtaining the band edge energies. A second slab calculation is required for obtaining the vacuum energy from the electrostatic potential profile along the vacuum direction. The relative band positions to vacuum were then deduced from the subtraction between the energies of slab band edges and the absolute vacuum energy.

Using HSE06-based computed electrostatic potential changes from bulk to surface with VASP, the absolute vacuum energy was obtained. Dipole corrections in the perpendicular direction to the surface were included to rectify possible errors that might occur from periodic boundary conditions.<sup>17</sup> More details about this scheme is reported in refs.<sup>18-20</sup>

Charge carrier transport properties are weighted by the electron/hole effective masses. Larger effective mass results in lower mobility and lower effective mass results in a higher mobility. As demonstrated in experiments,<sup>21-23</sup> the effective masses are required to be smaller than the free mass of electron to expect good charge carrier transport properties. Having useful information about any possible anisotropic nature of carriers present in the crystal lattice of the material can be obtained by the effective masses along different crystalline directions.

In the framework of the finite difference method,<sup>24</sup> the effective mass tensors for electrons  $(m_e^*/m_0)_{ij}$  and for holes  $(m_h^*/m_0)_{ij}$  were acquired from the HSE06-based  $k$ -space band structure. More details about this protocol is reported in refs.<sup>21,25-27</sup>

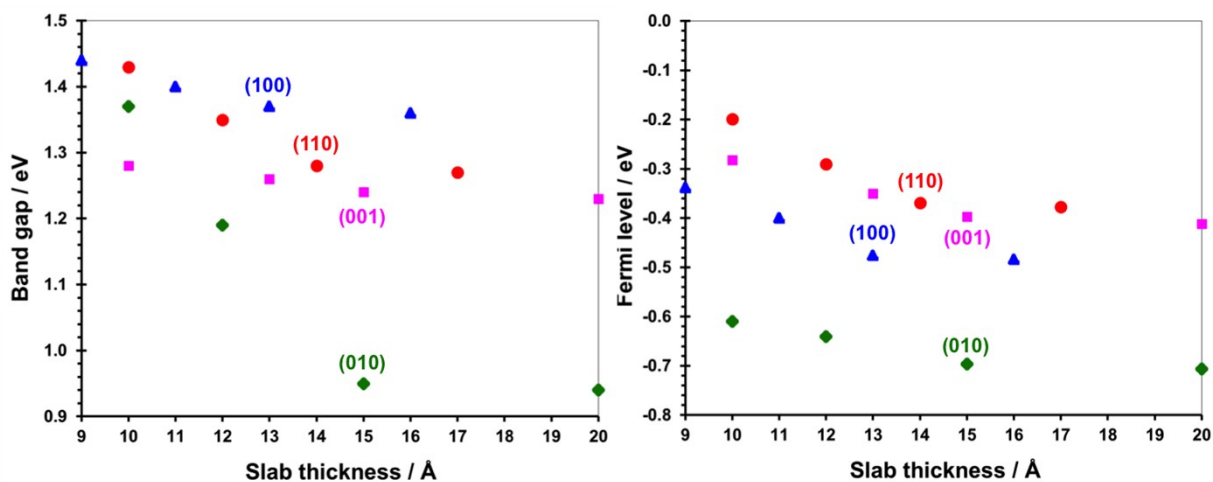


**Fig. S1** Benchmark convergence tests on the band gap value (left) and the Fermi level position (right) of the (110)-, (100)-, (010)-, and (001)-oriented pure  $\text{Ta}_3\text{N}_5$  slabs as a function of the crystal thickness obtained using the DFT/PBE method.

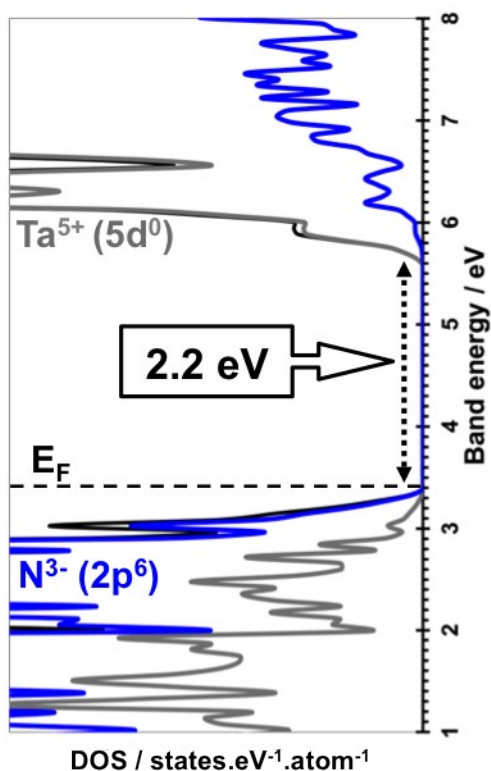


**Fig. S2** Electronic structure of bulk  $\text{Ta}_3\text{N}_5$  crystal obtained using the DFT/HSE06 method. Total DOS in black, partial DOS in light gray for Ti, in red for O, in dark gray for Ta, and in blue for N.

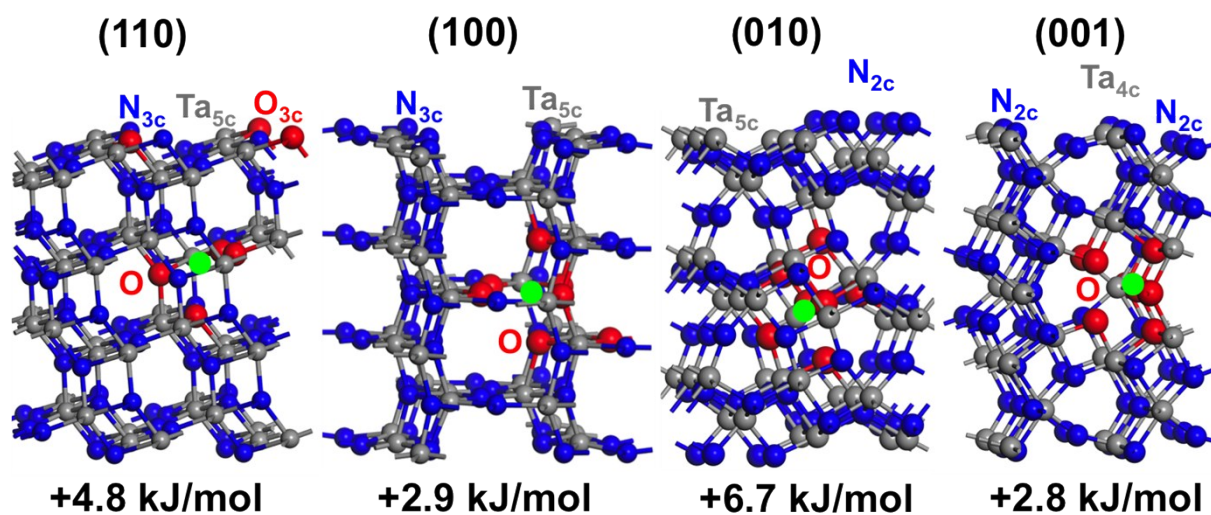


**Fig. S3** Metastable slab atomic structures together with their relative electronic energy to the most stable ones (in kJ/mol) for the four possible distinctive low-index (110), (100), (010), and (001) partial O-enriched  $Ta_3N_5$  surfaces obtained using the DFT/PBE method. Ta in dark gray, O in red, N in blue. The coordination numbers of surface and bulk O species are highlighted in each structure.

## References

- (1) Perdew, J. P.; Burke, K.; Ernzerhof, M. Generalized Gradient Approximation Made Simple. *Phys. Rev. Lett.* **1996**, *77*, 3865–3868.
- (2) Kresse, G.; Hafner, J. Ab Initio Molecular-Dynamics Simulation of the Liquid-Metal-Amorphous-Semiconductor Transition in Germanium. *Phys. Rev. B: Condens. Matter Mater. Phys.* **1994**, *49*, 14251–14269.
- (3) Kresse, G.; Furthmüller, J. Efficient Iterative Schemes for Ab-Initio Total-Energy Calculations Using a Plane-Wave Basis Set. *Phys. Rev. B: Condens. Matter Mater. Phys.* **1996**, *54*, 11169–11186.
- (4) Kresse, G.; Furthmüller, J. Efficiency of Ab-Initio Total Energy Calculations for Metals and Semiconductors Using a Plane-Wave Basis Set. *Comput. Mater. Sci.* **1996**, *6*, 15–50.
- (5) Kresse, G.; Joubert, D. From Ultrasoft Pseudopotentials to the Projector Augmented-Wave Method. *Phys. Rev. B: Condens. Matter Mater. Phys.* **1999**, *59*, 1758–1775.
- (6) Blöchl, P. E. Projector Augmented-Wave Method. *Phys. Rev. B* **1994**, *50*, 17953–17979.
- (7) Monkhorst, H, J.; Pack, J. D. Special Points for Brillouin-Zone Integration. *Phys. Rev. B* **1976**, *13*, 5188–5192.
- (8) Delley, B. From Molecules to Solids with the DMol3 Approach. *J. Chem. Phys.* **2000**, *113*, 7756–7764.
- (9) Delley, B. An All-Electron Numerical Method for Solving the Local Density Functional for Polyatomic Molecules. *J. Chem. Phys.* **1990**, *92*, 508–517.

- (10) Heyd, J.; Scuseria, G. E.; Ernzerhof, M. Hybrid Functionals Based on a Screened Coulomb Potential. *J. Chem. Phys.* **2003**, *118*, 8207–8215.
- (11) Heyd, J.; Scuseria, G. E.; Ernzerhof, M. Erratum: “Hybrid Functionals Based on a Screened Coulomb Potential” [J. Chem. Phys. 118, 8207 (2003)]. *J. Chem. Phys.* **2006**, *124*, 219906.
- (12) Van de Walle, C. G.; Martin, R. M. Theoretical Study of Band Offsets at Semiconductor Interfaces. *Phys. Rev. B* **1987**, *35*, 8154–8165.
- (13) Franciosi, A.; Van de Walle, C. G. Heterojunction Band Offset Engineering. *Surf. Sci. Rep.* **1996**, *25*, 1–140.
- (14) Rossmesl, J.; Skúlason, E.; Björketun, M. E.; Tripkovic, V.; Nørskov, J. K. Modeling the Electrified Solid-Liquid Interface. *Chem. Phys. Lett.* **2008**, *466*, 68–71.
- (15) Stevanovic, V.; Lany, S.; Ginley, D. S.; Tumasb, W.; Zunger, A. Assessing Capability of Semiconductors to Split water Using Ionization Potentials and Electron Affinities Only. *Phys. Chem. Chem. Phys.* **2014**, *16*, 3706–3714.
- (16) Pham, T. A.; Ping, Y.; Galli, G. Modelling Heterogeneous Interfaces for Solar Water Splitting. *Nat. Mater.* **2017**, *16*, 401–408.
- (17) Makov, G.; Payne, M. C. Periodic Boundary Conditions in Ab Initio Calculations. *Phys. Rev. B* **1995**, *51*, 4014–4022.
- (18) Harb, M.; Sautet, P.; Nurlaela, E.; Raybaud, P.; Cavallo, L.; Domen, K.; Basset, J.-M.; Takanabe, K. Tuning the Properties of Visible-Light-Responsive Tantalum (Oxy)Nitride Photocatalysts by Non-Stoichiometric Compositions: A First-Principles Viewpoint. *Phys. Chem. Chem. Phys.* **2014**, *16*, 20548–20560.

- (19) Harb, M.; Cavallo, L. Toward the Design of New Suitable Materials for Solar Water Splitting Using Density Functional Theory. *ACS Omega* **2018**, *3*, 18117–18123.
- (20) Harb, M.; Cavallo, L.; Basset, J.-M. Major Difference in Visible-Light Photocatalytic Features Between Perfect and Self-Defective Ta<sub>3</sub>N<sub>5</sub> Materials: A Screened Coulomb Hybrid DFT Investigation. *J. Phys. Chem. C* **2014**, *118*, 20784–20790.
- (21) Madelung, O. *Semiconductors: Data Handbook*, 3rd ed.; Springer: New York, 2004; pp 1–691.
- (22) Adashi, S. *GaAs and Related Materials*; World Scientific Publishing Co. Pvt. Ltd.: Singapore, 1994.
- (23) Vurgaftman, I.; Meyer, J. R.; Ram-Mohan, L. R. Band Parameters for III-V Compound Semiconductors and Their Alloys. *J. Appl. Phys.* **2001**, *89*, 5815–5875.
- (24) Fonari, A.; Sutton, C. Effective Mass Calculator for Semiconductors, <http://afonari.com/emc/> (accessed June 11, 2019).
- (25) Ziani, A.; Harb, M.; Noureldine, D.; Takanebe, K. UV-Visible Optoelectronic Properties of  $\alpha$ -SnWO<sub>4</sub>: A Comparative Experimental and Density Functional Theory Based Study. *Appl. Phys. Lett.* **2015**, *3*, 096101.
- (26) Noureldine, D.; Lardhi, S.; Ziani, A.; Harb, M.; Cavallo, L.; Takanebe, K. Combined Experimental-Theoretical Study of the Optoelectronic Properties of Non-Stoichiometric Pyrochlore Bismuth Titanate. *J. Mater. Chem. C* **2015**, *3*, 12032–12039.
- (27) Lardhi, S.; Noureldine, D.; Harb, M.; Ziani, A.; Cavallo, L.; Takanebe, K. Determination of Electronic, Dielectric and Optical Properties of Sillenite Bi<sub>12</sub>TiO<sub>20</sub> and

Perovskite-Like  $\text{Bi}_4\text{Ti}_3\text{O}_{12}$  Materials from Hybrid First-Principle Calculations. *J. Chem. Phys.*  
**2016**, *144*, 134702.